(a) Point cloud, concentrated around the straight line; $PHD \approx 1.0$

(b) Point cloud, concentrated around two curved intertwined lined; $PHD \approx 1.5$

Figure 7: An example of difference between intrinsic dimensionality (PHD) of a point clouds of different geometric shapes. The point cloud, concentrated around more complex structure (7b) has bigger PHD, than a point cloud, concentrated around simpler structure (7a)

A Theory

A.1 Formal definition of Persistent Homology

Persistent homology is a sequence of homology groups and linear maps parameterized by a filtration value. Here's the formal definition. Given a filtered chain complex (K, ∂) with filtration values $\lambda_1 < \lambda_2 < \ldots < \lambda_n$, we have a sequence of chain complexes: $K_{\lambda_0} \subseteq K_{\lambda_1} \subseteq K_{\lambda_2} \subseteq \ldots \subseteq K_{\lambda_n} = K$. For each λ_j, the i-th homology group $H_i(K_{\lambda_j})$ denotes the factor vector space $H_i(K_{\lambda_j}) = \ker \partial|_{K^{(i)}_{\lambda_j}} / \operatorname{im} \partial|_{K^{(i)}_{\lambda_j}}$. The inclusion $K_{\lambda_j} \subseteq K_{\lambda_{j+r}}$ induces a linear map $f_{j,j+r} : H_i(K_{\lambda_j}) \to H_i(K_{\lambda_{j+r}})$. By definition, Persistent Homology PH_i of the filtered chain complex is the collection of the homology groups $H_i(K_{\lambda_j})$, and the linear maps between them: $\mathrm{PH}_i = \{H_i(K_{\lambda_j}), f_{j,j+r}\}_{j,r}$.

By the structure theorem of persistent homology, a filtered chain complex (K, ∂) is decomposed into unique direct sum of standard filtered chain complexes of types $I(b_p, d_p)$ and $I(h_p)$, where $I(b, d)$ is the filtered complex spanned linearly by two elements e_b, e_d, $\partial e_d = e_b$ with filtrations $e_b \in I^{(i)}_b$, $e_d \in I^{(i+1)}_d$, $b \leq d$ and $I(h)$ is the filtered complex spanned by the single element $\partial e_h = 0$ with filtration $e_h \in I^{(i)}_h$. This collection of filtered complexes $I(b_p, d_p)$ and $I(h_p)$from the decomposition of K is called the $i-$th *Persistence Barcode* of the filtered complex K. It is represented as the multiset of the intervals $[b_p, d_p]$ and $[h_p, +\infty)$. In Section 3, when we speak loosely about the persistent homology PH_i, we actually mean the $i-$th persistence barcode. In particular the summation $\sum_{\gamma \in \mathrm{PH}_i}$ is the summation over the multiset of intervals constituting the $i-$th persistence barcode.

A.2 Equivalence between PH_0(S) and MST(S)

For the convenience of the reader, we provide a sketch of the equivalence between the 0-th persistence barcodes and the set of edges of minimal spanning tree (MST).

First, recall the process of building of 0-dimensional persistence barcode Adams et al. (2020). Given a set of points S, we consider a simplicial complex K, consisting of points and all edges between them (we don't need to consider faces of higher order for H_0 computation): $K = \{S\} \cup \{(s_i, s_j) | s_i, s_j \in S\}$. Each element in the filtration $K_{\lambda_0} \subseteq K_{\lambda_1} \subseteq K_{\lambda_2} \subseteq \ldots \subseteq K_{\lambda_n} = K$ contains edges shorter than the threshold λ_k: $K_{\lambda_k} = \{S\} \cup \{(s_i, s_j) | s_i, s_j \in S, ||s_i - s_j|| < \lambda_k\}$. The 0-th persistence barcode is the collection of lifespans of 0-dimensional features, which correspond to connected components, evaluated with growths of the threshold λ. Let's define a step-by-step algorithm of the features' lifespans evaluation. We are starting from $\lambda = 0$, when each point is the connected component, so all the features are born. We will add edges to the complex in increasing order. On each step, we are given a set of connected components and a queue of the remaining edges ordered by length. If the next edge of the length λ connects two of the connected components to each other, we claim the $death$ of the first component, and add a new lifespan $(0, \lambda)$ to the persistence barcode; otherwise, we just remove the edge from the queue; its addition to the complex does not influence the $0-$th barcode.

Now, we can notice, that this algorithm exactly corresponds to the classical Prime's algorithm for MST building, where the appearance of a new bar $(0, \lambda)$ corresponds to adding the edge of the length λ to MST.

B Algorithm for PHD computation

In Section 4 of the paper we described a general scheme for computation of Persistence Homology Dimension. Here we give a more detailed explanation of the algorithm.

Input: a set of points S with $|S| = n$.

Output: $\dim^0_{PH}(S)$.

1. Choose $n_i = \frac{(i-1)(n-\hat{n})}{k} + \hat{n}$ for $i \in \overline{1, \dots k}$; hence, $n_1 = \hat{n}$ and $n_k = n$. Value of k may be varied, but we found that $k = 8$ is a good trade-off between speed of computation and variance of PHD estimation for our data (our sets of points vary between 50 and 510 in size). As for $\hat{n}$, we always used $\hat{n} = 40$.
2. For each i in $1, 2, \dots k$
   (a) Sample J subsets $S_i^{(1)}, \dots S_i^{(J)}$ of size n_i. For all our experiments we took $J = 7$.
   (b) For each $S_i^{(j)}$ calculate the sum of lengths of intervals in the 0th persistence barcode $E_0^1(S_i^{(j)})$.
   (c) Denote $E(S_i)$ as median of $E_0^1(S_i^{(j)}), j \in \overline{1, \dots J}$.
3. Prepare a dataset consisting of k pairs $D = \{(\log n_i, \log E(S_i))\}$ and apply linear regression to approximate this set by a line. Let κ be the slope of the fitted line.
4. Repeat steps 2-3 two more times for different random seeds, thus obtaining three slope values κ_1, κ_2, κ_3 and take final κ_F as their average.
5. Estimate the dimension d as $\frac{1}{1-\kappa_F}$

C Additional experiments

C.1 Choice of some parameters in the formula for PHD

As was mentioned in Section 3, we estimate value of Persistance Homology Dimension from the slope of the linear regression between $\log E^0_\alpha(X_{n_i})$ and $\log n_i$. Thus, the exact value of PHD of a text actually depends on the non-negative parameter α. The theory requires it to be chosen less than the intrinsic dimension of the text, and in all our experiments we fix $\alpha = 1.0$.

Figure 8 shows how exact value of PHD of a natural and generated texts (of approximately same length) depends on the choice of α.

Nonetheless, choice $\alpha = 1.0$ seems to yield reasonable performance, but further investigations of this issue are required.

For $\alpha \in [0.5; 2.5]$ our results, in general, lie in line with experiments from Birdal et al. (2021), where performance of $\dim^0_{PH}$ with α varying between 0.5 and 2.5 was studied on different types of data.

C.2 Effect of paraphrasing on intrinsic dimension

As we show in paragraph *Comparison with universal detectors experiments* from Section 4, usage of paraphrasing tools cause little effect on PHD-based detector ability to capture difference between

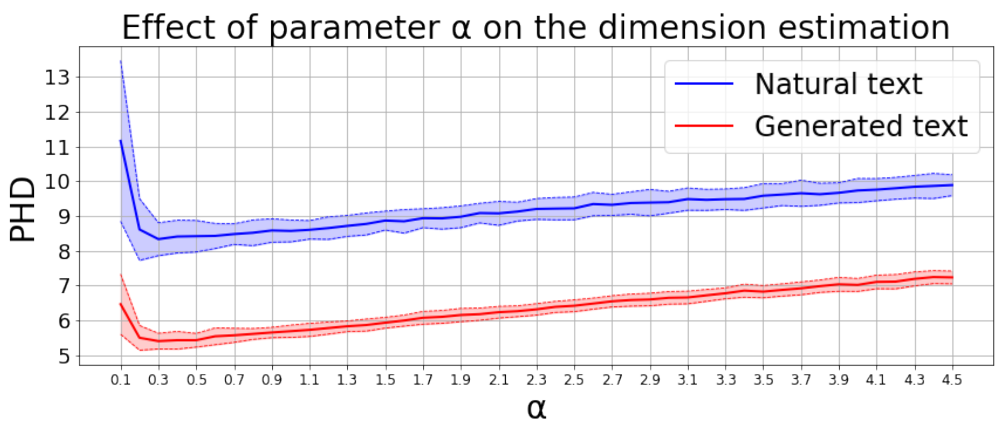

Figure 8: PHD estimates at various α for a natural and a generated texts.

Table 5: Effect of paraphrasing on the intrinsic dimension of the text. Here we can see an uncommon example of data where MLE and PHD behave differently — paraphrasing do not pose much trouble for PHD (its quality even increases marginally), but the performance of MLE-based detector is decreased significantly, especially for GPT-3.5.

Method	Original	DIPPER parameters					
		Lex 20	Lex 20 Order 60	Lex 40	Lex 40 Order 60	Lex 60	Lex 60 Order 60
PHD	7.30 $\pm$1.66	7.33 $\pm$1.69	7.35 $\pm$1.16	7.42 $\pm$1.69	7.45 $\pm$1.78	7.51 $\pm$1.76	7.51 $\pm$1.72
MLE	9.68 $\pm$1.31	9.91 $\pm$1.22	9.90 $\pm$1.24	9.97 $\pm$1.22	9.95 $\pm$1.21	10.00 $\pm$1.18	10.01 $\pm$1.15

generated and natural texts. Here show how such tampering with generated sentences affects their intrinsic dimension. Table 5 presents the mean values of PHD and MLE after applying DIPPER with different parameters to the generation of GPT-3.5 Davinci. Where value of Order (re-ordering rate) is not specified it means it was left at default value 0. Both parameters, Lex (lexical diversity rate) and Order can vary from 0 to 100; for additional information please refer to , where DIPPER was introduced.

Increase in lexical diversity entails slight grows of both mean PHD and mean MLE that, in theory, should make our detectors less efficient. In case of PHD-based detector we do not observe this decrease in performance, probably due to the mean shift being indeed rather small and caused mostly by the right tail of the distribution — the texts that even before paraphrasing have high chance of evading detection.

Meanwhile, increase of the re-ordering rate from 0 to 60 has almost no noticeable impact.

C.3 Non-native speaker bias

Here we present full results for our experiments on bias of ML-based artificial text detectors. On Figure 9 we present baseline results for all detectors studied in Liang et al. (2023) that were not included into main text of our article

C.4 Intrinsic dimension of texts in different languages

Figure 10 presents PHD of natural and generated texts in different languages on data from Wikipedia. Embedding were obtained from the same multilingual model XLM-RoBERTa-base.

D Examples of generated texts

Table 6: Examples of original text and text generated by ChatGPT. The common prompt parts are highlighted in bold.

Original (English)	Generated (English)
USS Mills (DE-383) **World War II North Atlantic operations** **After shakedown out of Bermuda, Mills trained nucleus crews for frigates and destroyer escorts off Norfolk, Virginia, until 10 January 1944 when she began transatlantic convoy escort duty.** On her second voyage into the Mediterranean, Mills' convoy was attacked before dawn 1 April 1944, 56 miles west of Algiers by German torpedo bombers. SS Jared Ingersoll, a Liberty ship, was hit and set blazing. Mills picked up survivors who had abandoned ship, and sent a boarding party to extinguish her fires. British tug HMS Mindfull and Mills then towed Jared Ingersoll to Algiers.	**USS Mills (DE-383)** **World War II North Atlantic operations** **After shakedown out of Bermuda, Mills trained nucleus crews for frigates and destroyer escorts off Norfolk, Virginia, until 10 January 1944 when she began transatlantic convoy escort duty.** The Mills escorted her first two convoys in January and February from New York City to the United Kingdom, making four round trip crossings by May 1944. During her North Atlantic operations, Mills successfully thwarted several attacks by German U-boats, and carried out rescue operations for nearby ships in distress. She also participated in sweeping the area for mines in preparation for the Normandy invasion.
Original (Spanish)	Generated (Spanish)
Currulao **Instrumentos** **Si la música involucra el uso de una chirimia que es popular en la costa norte, específicamente en el Chocó: Tambor tambora, Cununos ("macho" y "hembra") y un clarinete.** Esta agrupación también puede incluir un eufonio que, en algunos casos, reemplaza o acompaña a un saxofón. Si se trata de un grupo de marimba que es popular en el sur de la región, específicamente al sur del Chocó, Valle del Cauca, Cauca y Nariño: la marimba de chonta, los cununos ("hembra" y "macho"), guasá y el tambor bajo.	**Currulao** **Instrumentos** **Si la música involucra el uso de una chirimia que es popular en la costa norte, específicamente en el Chocó: Tambor tambora, Cununos ("macho" y "hembra") y un clarinete.** El currulao es una danza musical tradicional originaria de la región de la costa Pacífica de Colombia, la cual se deriva de la mezcla de las culturas africana, indígena y española. El sonido del currulao es único y se distingue por el uso de instrumentos que le otorgan su ritmo y cadencia característicos.
Original (Polish)	Generated (Polish)
Juan Machuca **Kariera klubowa** **Całą karierę piłkarską Juan Machuca spędził w klubie Unión Española, w którym występował w latach 1969-1987.** Z Unión Española trzykrotnie zdobył mistrzostwo Chile w 1973, 1975 i 1977. Na arenie międzynarodowej dotarł do finału Copa Libertadores 1975, w którym Unión uległ argentyńskiemu Independiente Avellaneda.	**Juan Machuca** **Kariera klubowa** **Całą karierę piłkarską Juan Machuca spędził w klubie Unión Española, w którym występował w latach 1969-1987.** Był to okres, w którym klub ten odnosił wiele sukcesów, m.in. zdobył mistrzostwo Chile w 1973 i 1975 roku oraz Puchar Chile w 1975 roku.

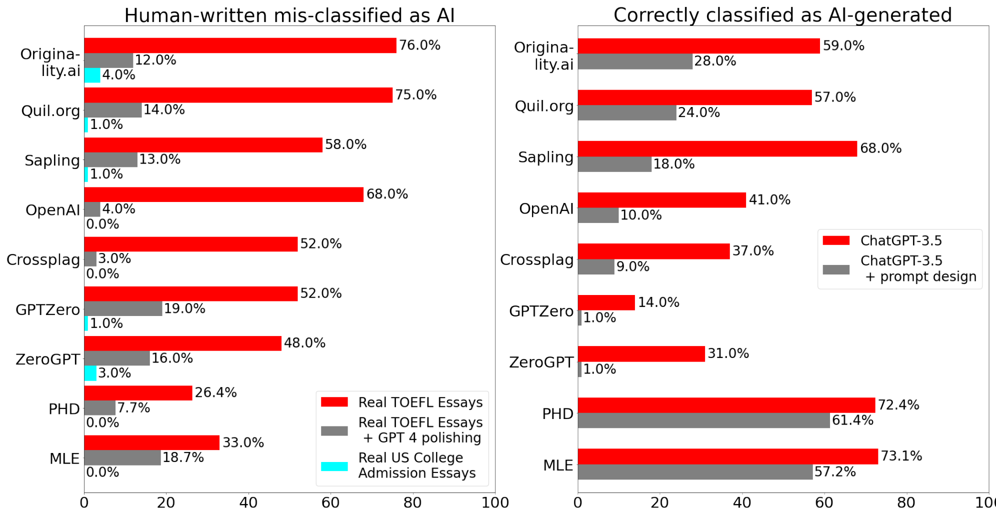

Figure 9: Comparison of GPT detectors in non-standard environment. Left: bias against non-native English writing samples. Right: decrease in performance due to prompt design.

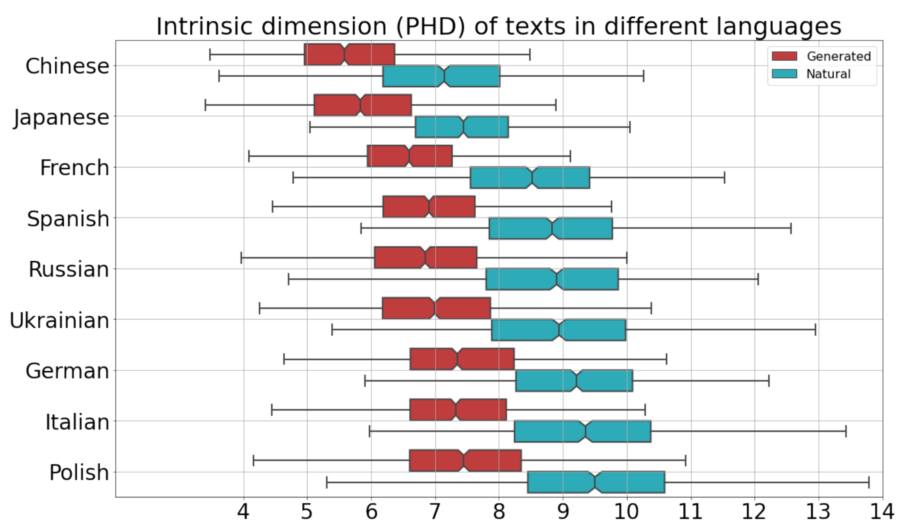

Figure 10: Boxplots of PHD distributions in different languages on Wikipedia data. Embeddings are obtained from XLM-RoBERTa-base (multilingual).